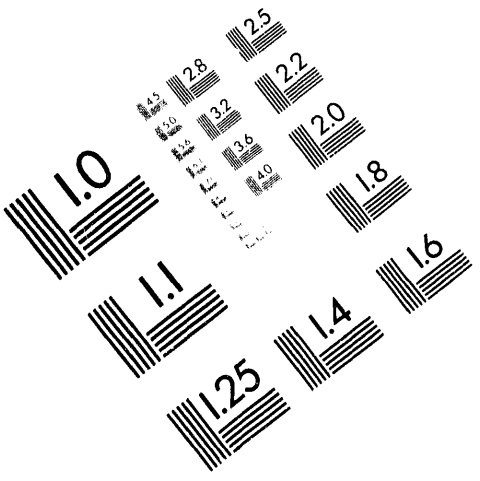

Association for Information and Image Management

1100 Wayne Avenue, Suite 1100
Silver Spring, Maryland 20910

301/587-8202

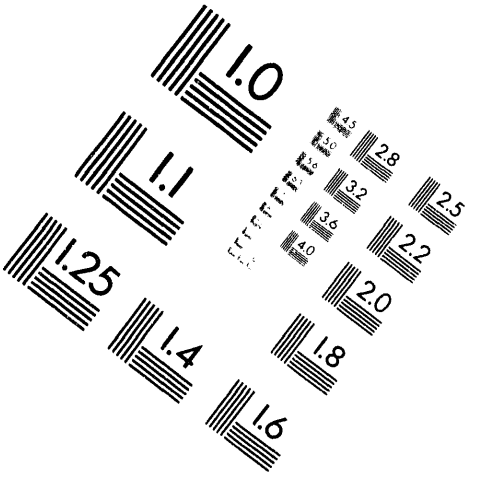

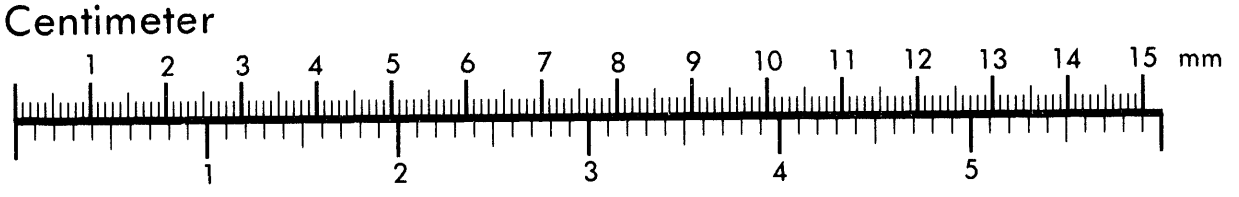

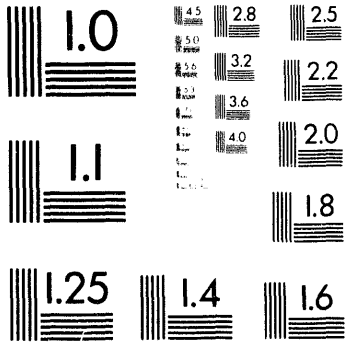

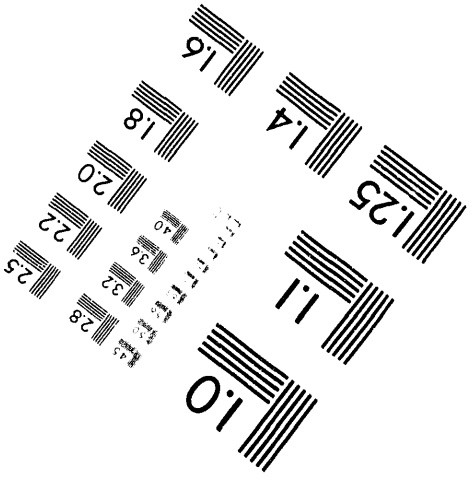

MANUFACTURED TO AIIM STANDARDS
BY APPLIED IMAGE, INC.

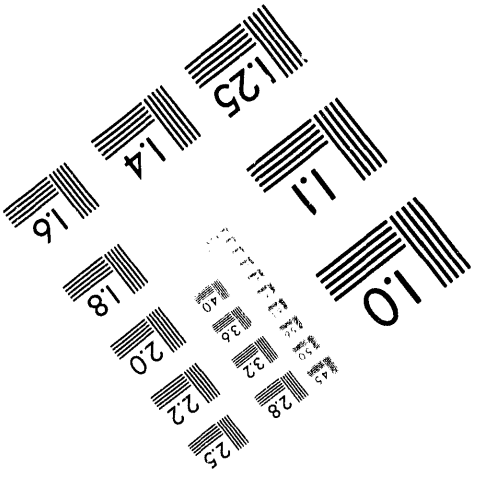

1 of 1

MHD-FLOW IN SLOTTED CHANNELS WITH CONDUCTING WALLS

Igor A. Evtushenko, Igor R. Kirillov
D.V. Efremov Scientific Research Institute of Electrophysical Apparatus
St. Petersburg, 189631, Russia

Claude B. Reed
Argonne National Laboratory, Chicago, IL 60439, USA

MS 021

July 1994

DISCLAIMER

Paper presented at the 3rd International Symposium on Fusion Nuclear Technology, Los Angeles, CA, June 27-July 1, 1994

*Work supported by the U.S. Department of Energy, Office of Fusion Energy, under Contract W-31-109-Eng-38.

MHD-FLOW IN SLOTTED CHANNELS WITH CONDUCTING WALLS

Igor A. Evtushenko, Igor R. Kirillov
D.V. Efremov Scientific Research Institute of Electrophysical Apparatus
St. Petersburg, 189631, Russia

Claude B. Reed
Argonne National Laboratory, Chicago, IL 60439, USA

Abstract

A review of experimental results is presented for magnetohydrodynamic (MHD) flow in rectangular channels with conducting walls and high aspect ratios (longer side parallel to the applied magnetic field), which are called slotted channels. The slotted channel concept was conceived at Efremov Institute as a method for reducing MHD pressure drop in liquid metal cooled blanket design. The experiments conducted by the authors were aimed at studying both fully developed MHD-flow, and the effect of a magnetic field on the hydrodynamics of 3-D flows in slotted channels. Tests were carried out on five models of the slotted geometry.

A good agreement between test and theoretical results for the pressure drop in slotted channels was demonstrated. Application of a "one-electrode movable probe" for velocity measurement permitted measurement of the M-shape velocity profiles in the slotted channels. Suppression of 3-D inertial effects in slotted channels of complex geometry was demonstrated based on potential distribution data.

1. Introduction

A review of test results is presented in support of the slotted channel concept, Lavrentiev [1] conceived at Efremov Institute as a method for MHD pressure reduction. Five rectangular channels with conducting walls and high aspect ratios (ratio of channel's cross-section dimensions), referred to as slotted channels or channels of slotted geometry, were tested. Experimental conditions and test section geometry are summarized in Table 1. Detailed descriptions of the test models and test conditions can be found in references [2,3,4].

2. Fully Developed Flows in Slotted Channels

2.1 Pressure Drop

Comparison of the experimental data and theoretical predictions for pressure drop in fully developed MHD-flows in slotted channels 1, 2, and 3 is presented in Table 2. The data for channels 1 and 2 are compared with the analytical dependence of K. Miyazaki [5]. For channel 3, the comparison is made with Argonne National Laboratory (ANL) numerical calculations based on the core flow approximation.

The comparison of data on the pressure drop in channel 3 in which the "laminated walls" technology was applied suggests workability of such technology. The reduction of pressure caused by the application of three laminated walls (1 mm in thickness) electrically insulated from their strongback (6 mm in thickness) is about the ratio of thicknesses.

The peculiarity of MHD-flow in slotted channel is its high sensitivity to the magnetic field inclination. The pressure drop in channel 2, when the channel is inclined 6 ° (the angle characteristic of fusion reactor blankets) to the magnetic field, is about 1.3 times the pressure drop in both uniform and nonuniform magnetic fields that are not inclined to the flow.

2.2 Velocity Profiles

The velocity profile in slotted channels with conducting walls and sufficiently high Hartmann numbers is M-shaped, Fig. 5. The maximum velocities and the largest velocity gradients are located in a narrow, 2-3 mm zone, under the conditions of this study. Thus, the spatial resolution of the probes becomes a key issue. The spatial resolution of traditional, two-electrode probes with separation of about 1-1.5 mm (for example, the Thermal Liquid-Metal Electromagnetic Velocity Instrument (TLEVI) probe with tip separation of 0.88 mm and the tip (thermocouple) diameter of 0.5 mm applied in the experiment on channel 3) is about 30-75% of the size of the maximum velocity zone. And thus, such probes do not permit acquisition of reliable data on the velocity profiles.

Evidently, more reliable measurements could be acquired with a one-electrode probe. In this case the potential difference $\Delta\varphi(z)$ is measured between the moving electrode of the probe and an electrode on the channel wall. Then, the velocity profile could be defined by the differentiation of the potential distribution along the direction perpendicular to the applied magnetic field: $v(z) = B^{-1} \cdot \partial(\Delta\varphi(z))/\partial z$. The spatial resolution of such a method is defined by the method of experimental data approximation and numerical differentiation. This method of velocity measurement was used in the experiments on channel 2. Comparison of

experimental data and numerical predictions, Sidorenkov and Shishko [6] on velocity presented in Fig. 5 suggests that the method is workable. The 0.2-0.6 mm (in different experiments) shift of experimental velocity profiles in comparison to the theoretical ones could be caused by two reasons: (1) an error in determination of the distance from the wall and (2) a difference between the test channel geometry and the channel geometry used in theoretical analysis - test channel 2 had rounded corners.

3. 3-D MHD Flows in Channels of Slotted Geometry

3.1 Hydraulics of the Flow in a Slotted Channel with Anchor Links

Experimental studies of MHD-flow in a slotted channel with anchor links (cylinders installed inside the channel along its centerline and perpendicular to the magnetic field for the purpose of decreasing the mechanical stresses in sidewalls) were carried out on channels 1 and 3, with 5 and 6 cylinders, respectively, installed along the channel axes. The wall conductivity ratio for the cylinder walls was the same as that of the Hartmann walls of the channel. The data on the pressure drop over a length equal to the channel width 2b are presented in Table 3.

The agreement of the pressure drop ratio measurements for the two channels with different wall conduction ratios, but similar geometry, suggests that the additional pressure drop is caused mainly by the decrease in flow area caused by the anchor links. Due to the large additional pressure drop caused by the anchor links, a 6 ° inclination of the magnetic field had almost no additional effect on the pressure drop in channel 1 with anchor links. It should be mentioned that the pressure drop ratios presented in Table 3 are valid for high interaction parameters and are nearly

independent of the Hartmann number. At small N, the 3-D effects produce the following pressure drop dependence on the Hartmann number: $\Delta p/N \cdot \rho V^2 = \beta_0 + \beta_1 M^{-1}$.

3.2 The Effect of the Magnetic Field on 3-D Flow in Channels of Slotted Geometry

Due to the large pressure drop caused by the conducting walls, the application of methods based on the analysis of pressure drops to study the effect of a magnetic field on 3-D inertial effects in channels with conducting walls, is troublesome, compared to channels with insulating walls. Therefore, in the tests reported here, the effect of the magnetic field on 3-D effects was determined based mainly on the potential distribution data.

Suppression of inertial 3-D effects in channels with anchor links should lead to a decrease in the asymmetry of the flow around the anchor links and to potential distributions which are independent of the interaction parameter. Data presented in Fig. 6 for channel 3 show that the downstream electrode distributions do not vary with interaction parameters above N>1000; but the upstream electrode distributions depend on N even at the highest interaction parameters achieved in the experiment, although the tendency toward suppression of 3-D effects is quite apparent in this area. Qualitatively, the same effect was observed in the downstream and upstream anchor link areas of channel 1. These results suggest that the transition to non-inertial flow in the magnetic field should not be considered as a process occurring under the same conditions (MHD-parameters) in the whole area of 3-D flow, but should be deemed as a local process.

The asymmetry coefficient of potential distributions around an anchor link is shown in Fig. 7 as a function of interaction parameter for three experiments (channels 1, 3, and channel 1 with insulating walls). The asymmetry coefficient is defined as follows, Korn and Korn [7]:

$$\gamma_{asym} = \sum_i (x_i - x_0)^3 \, \Delta\varphi_i \Big/ \left[\sum_i (x_i - x_0)^2 \, \Delta\varphi_i\right]^{3/2} ,$$

where $x_0 = \sum_i x_i \Delta\varphi_i$ is the normalized potential difference at $x=x_i$.

Although it is difficult to make general conclusions, one can see from Fig. 7 that the asymmetry coefficient strongly depends on the relative electrical conductivity of the channel walls. As for the coefficient's dependence on N, in the general case, one should first expect an increase in γ_{asym} with increasing N due to the influence of adjacent anchor links; then a decrease in γ_{asym} with further increasing N due to the suppression of 3-D effects and the decrease in influence of adjacent links; and finally, a small decrease in γ_{asym} due to the suppression of 3-D effects around one "isolated" link. The higher the relative conductivity of the side walls, the greater the values of the interaction parameter at which the reduction of γ_{asym} takes place. This is obviously related to the increase in the length of stabilized flow in up- and downstream anchor link areas with increasing "c" and, with the increase in interaction between the nearby anchor links.

The asymmetry coefficient was also applied in the study of magnetic field influence on the inertial 3-D effects in channel 4. The data on the asymmetry coefficient:

$$\gamma^1_{asym} = [(\Delta\varphi_4 - \Delta\varphi_1)^2 - (\Delta\varphi_3 - \Delta\varphi_2)^2]^{1/2} / \sqrt{2}$$

of the potential distribution ($\Delta\varphi_i$, $i=1\text{-}4$, the measured potential differences on the opposite side walls in the mid-cross section of the channel) show that an increase in the magnetic field leads to quick suppression of the entry effects (Fig. 8) caused by the 90 °-bend and the transition from circular geometry to the slotted one. At high interaction parameters, the asymmetry coefficient tends to zero, which means that the flow in the mid-cross section is almost fully developed at high values of N.

The suppression of inertial effects was also observed in channel 5. The quantitative structure of the flow at different interaction parameters, based on the potential difference measurements between side walls, shows the following. When the interaction parameter is first increased, a large-scale vortex-type flow, generated in an area of abrupt expansion (Fig. 9a), is divided into two vorticies of small size (Fig. 9b). Further increase in the interaction parameter leads to full suppression of the vortex in the central area of the channel, and to the decrease of the vortex localized in the corner of the channel (Fig. 9c).

4. Conclusions

1. Comparison of experimental data and theoretical predictions on pressure drop in slotted channels shows that the pressure drop can be estimated with sufficient accuracy by existing analytical and numerical approaches.

2. M-shaped velocity profiles, forming in slotted channels at high Hartmann numbers, can be measured by a one-electrode probe.

3. Experimental data on pressure drop reduction due to the application of laminated wall technology shows the workability of this technology.

4. Test data on the influence of the magnetic field on 3-D effects show that although an increase in the magnetic field generally leads to the suppression of inertial effects, the specific features of the process depend not only on the values of the Hartmann number and interaction parameter, but also on the channel geometry, wall conduction ratio, and the local characteristics of the flow. Thus, it is not possible to define general conditions for transition to inertialess flow in slotted channels at this time.

Nomenclature

B	-	magnetic field strength
a	-	half depth of a channel perpendicular to the B direction
b	-	half width of a channel in the B direction
M	-	Hartmann number $=Ba\sqrt{\sigma/\rho\nu}$
N	-	interaction parameter $(= \sigma B^2 a/\rho V)$
c	-	wall conduction ratio $(= \sigma_w t_w/\sigma a)$
k_p	-	pressure drop coefficient $(= (dp/dz)/\sigma B^2 V)$
Re	-	Reynolds number $(= V \cdot a/\nu)$
p	-	pressure
φ	-	potential
V	-	velocity
ρ	-	density
σ	-	electrical conductivity
ν	-	viscosity

Subscripts

H.W.	-	Hartmann wall
S.W.	-	Side wall

References

1. I.V. Lavrentiev, Liquid metal blanket of fusion tokamak reactor, in: IV All Union Conference on the Engineering Problems of Fusion Reactors, Leningrad (1988) pp. 326-327.

2. I.A. Evtushenko, A.T. Kusainov, K. MacCarthy, S.I. Sidorenkov and A.V. Tananaev, Magnetohydrodynamic flow in the channel with a periodical system of cylinders. Part I. Experimental results, Magnitnaya Gidrodynamika 1 (1992), 60-64.

3. C.B. Reed, T.Q. Hua, D.B. Black, I.R. Kirillov, S.I. Sidorenkov et al., Liquid metal MHD and heat transfer in a tokamak blanket slotted coolant channel, Proceedings IEEE/NPSS Fusion 15th Symposium on Fusion Engineering, Hyannis, MA (1993).

4. I.A. Evtushenko, S.I. Sidorenkov and A. Ya. Shishko. Experimental study of the MHD processes in the slotted channels in a strong magnetic field, Magnitnaya Gidrodynamika 2 (1993) 83-94.

5. K. Miyazaki, Research activity on liquid metal MHD for advanced nuclear power systems, presented at Japan-CIS Seminar on Liquid Metal MHD, Tokyo (May 1992).

6. S.I. Sidorenkov and A. Ya. Shishko. Variational method of Magnetohydrodynamics flows calculations in the slotted channel with conducting walls, Magnitnaya Gidrodynamika 4 (1991) 87-96.

7. G.A. Korn, T.M. Korn. Mathematical Handbook for Scientists and Engineers. McGraw-Hill Book Company, Inc., N.Y., Toronto, London, 1961.

Table 1.

Channel No. / Fig.	Geometry	Aspect ratio 2a/2b (mm/mm)	Wall conduction ratio $c_{H.W.}/c_{S.W.}$	Hartmann number M	Interaction parameter N
1 Fig. 1	straight channel with and without anchor links	10 / 100	0.19 / 0.19	50 - 170	2 - 100
2 Fig. 1	straight channel	10 / 100	0.46 / 0.46	50 - 120	10 - 80
3 Fig. 2	straight channel with and without anchor links	14 / 140	0.07 - laminated walls/0.42	400, 800	100 - 8800
4 Fig. 3	90°-bend and transition from circular to slotted channel	7 / 70	0.24 / 0.0	200 - 1000	2 - 240
5 Fig. 4	abrupt expansion	7 / 350	0.24 / 0.0	200 - 1000	2 - 2000

Table 2.

Channel	Hartmann number	$k_p^{exper.} / k_p^{theor.}$
1	115	0.91
2	90-120	1.02
3	400 800	1.15-1.30 1.10-1.25

Table 3.

Channel	Anchor link diameter (mm)	Anchor link separation (mm)	Magnetic field inclination	$\frac{\Delta p_{with}}{\Delta p_{without}}$
1	10	100	0°, 6°	1.6 - 1.8
3	15	140	0°	1.6 - 1.75

Figure Captions

Fig. 1 Slotted channels 1 and 2 geometry

Fig. 2 Slotted channel 3 geometry

Fig. 3 Slotted channel 4 geometry

Fig. 4 Slotted channel 5 geometry

Fig. 5 Normalized velocity profile in slotted channel 2 (v/V)

Fig. 6 Axial distribution of bottom electrode voltages along test section centerline upstream and downstream of an anchor link

Fig. 7 Asymmetry of axial potential distributions in a channel with anchor links (experiment)

Fig. 8 Asymmetry of the potential difference distribution in channel 4

Fig. 9 The effect of the magnetic field on the 3-D effects in channel 5: Re=2100, a) M=136; b) M=410; c) M=545

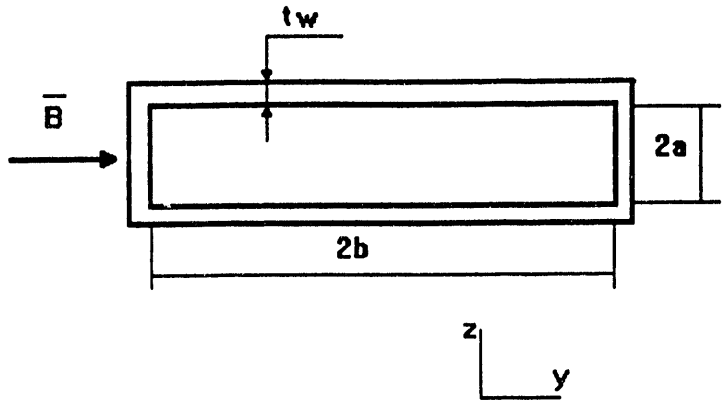
tw
B
2a
2b
z
y

Fig.1

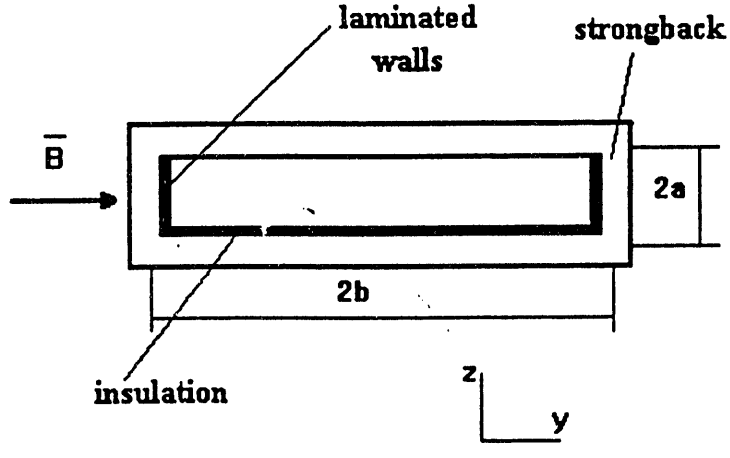
laminated
walls
strongback
B
2a
2b
insulation
z
y

Fig.2

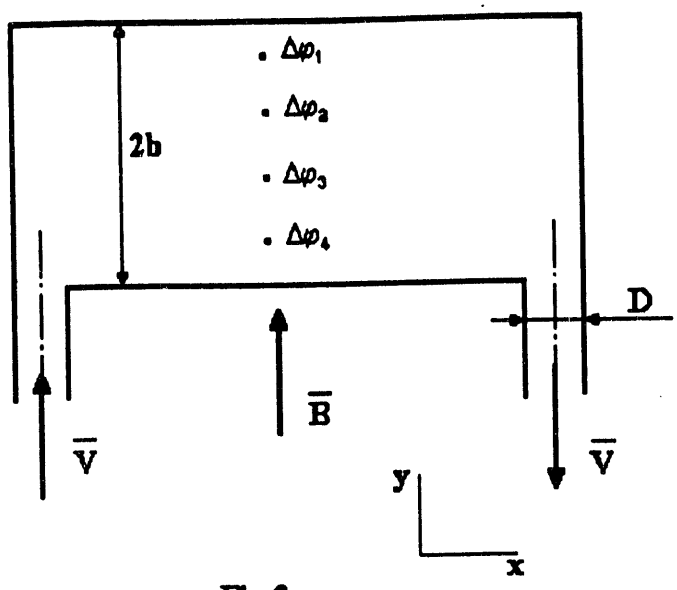
$\Delta\varphi_1$
$\Delta\varphi_2$
$\Delta\varphi_3$
$\Delta\varphi_4$
2b
D
$\overline{B}$
$\overline{V}$
$\overline{V}$
y
x

Fig.3

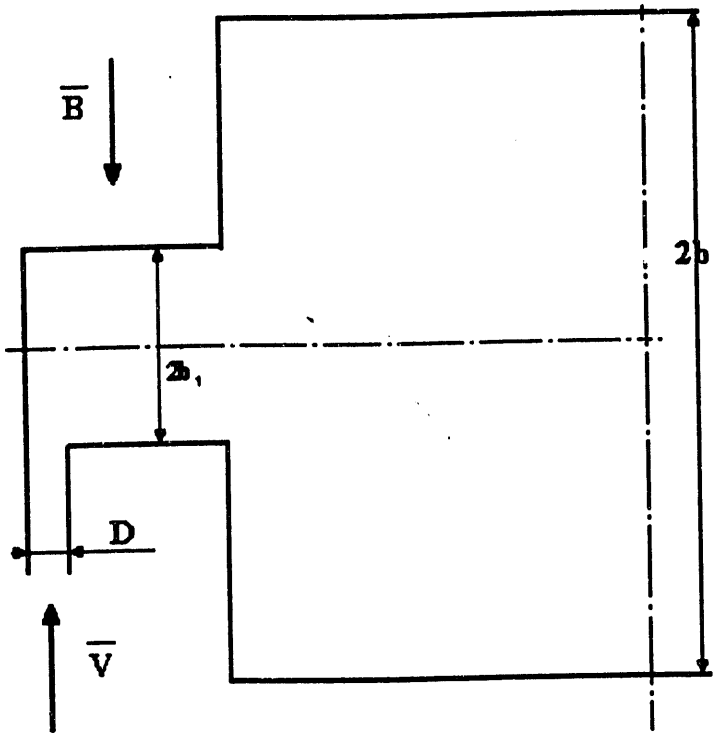
$\overline{B}$
2b
$2b_1$
D
$\overline{V}$

Fig.4

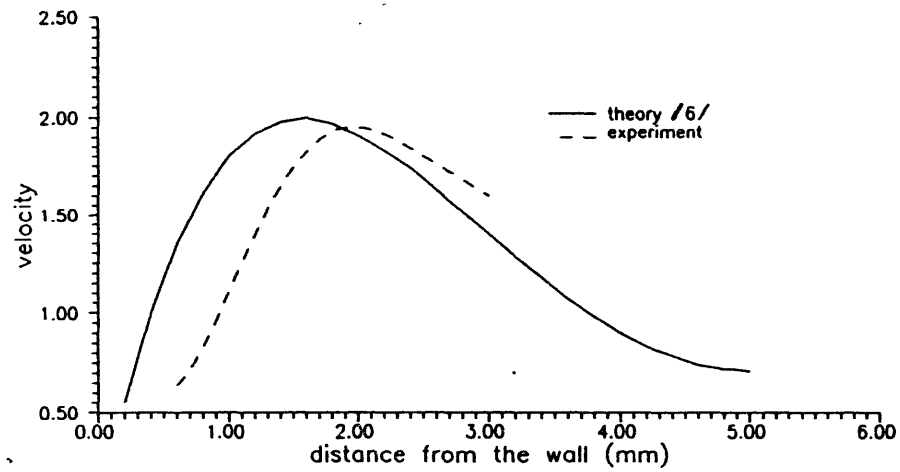
2.50
2.00
1.50
1.00
0.50
velocity
0.00
1.00
2.00
3.00
4.00
5.00
6.00
distance from the wall (mm)
theory /6/
experiment

Fig. 5

FIGURE 6

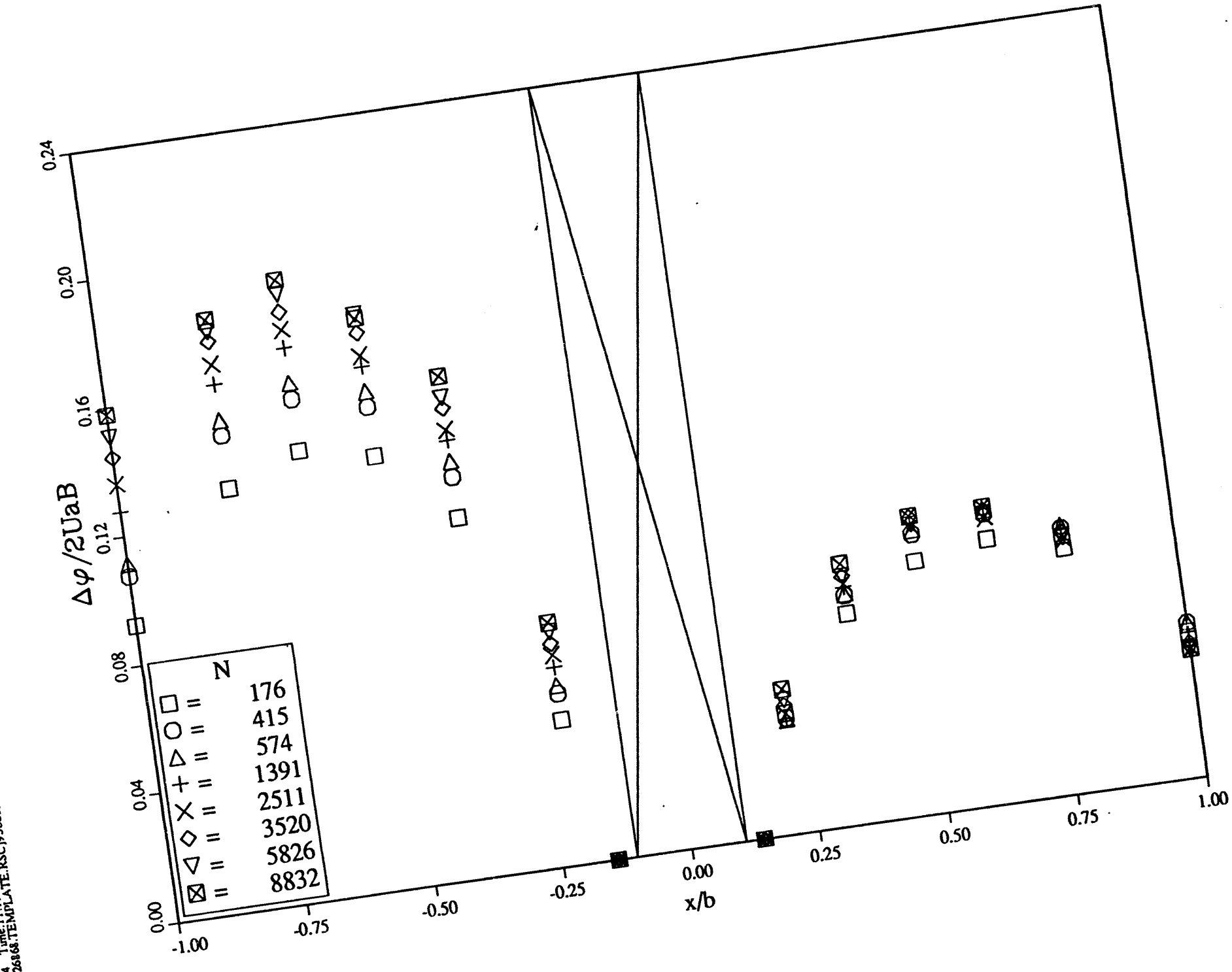

Date: 8/ 2/94 Time: 11:11:10 User:{ALEX.B26868}
$DISK1:[B26868.TEMPLATE.RSC]930602AA_ELECTRODES.TEMPLATE;10

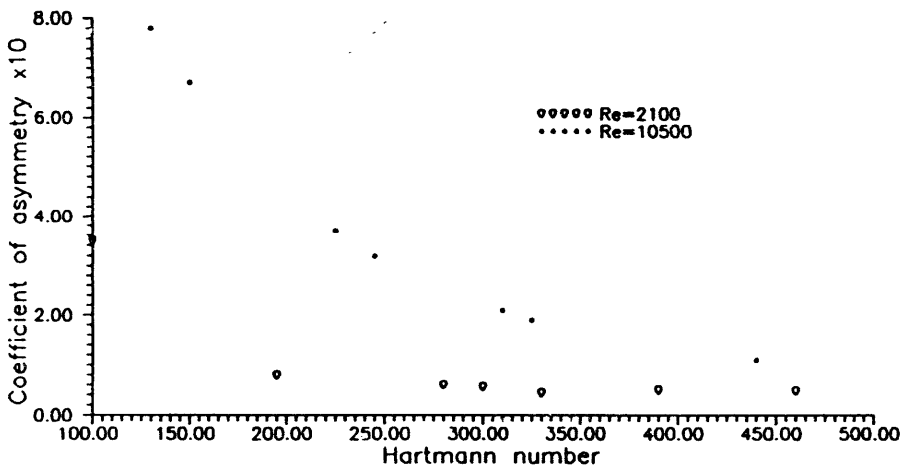
8.00
6.00
4.00
2.00
0.00
Coefficient of asymmetry x10
100.00
150.00
200.00
250.00
300.00
350.00
400.00
450.00
500.00
Hartmann number
Re=2100
Re=10500

Fig. 8

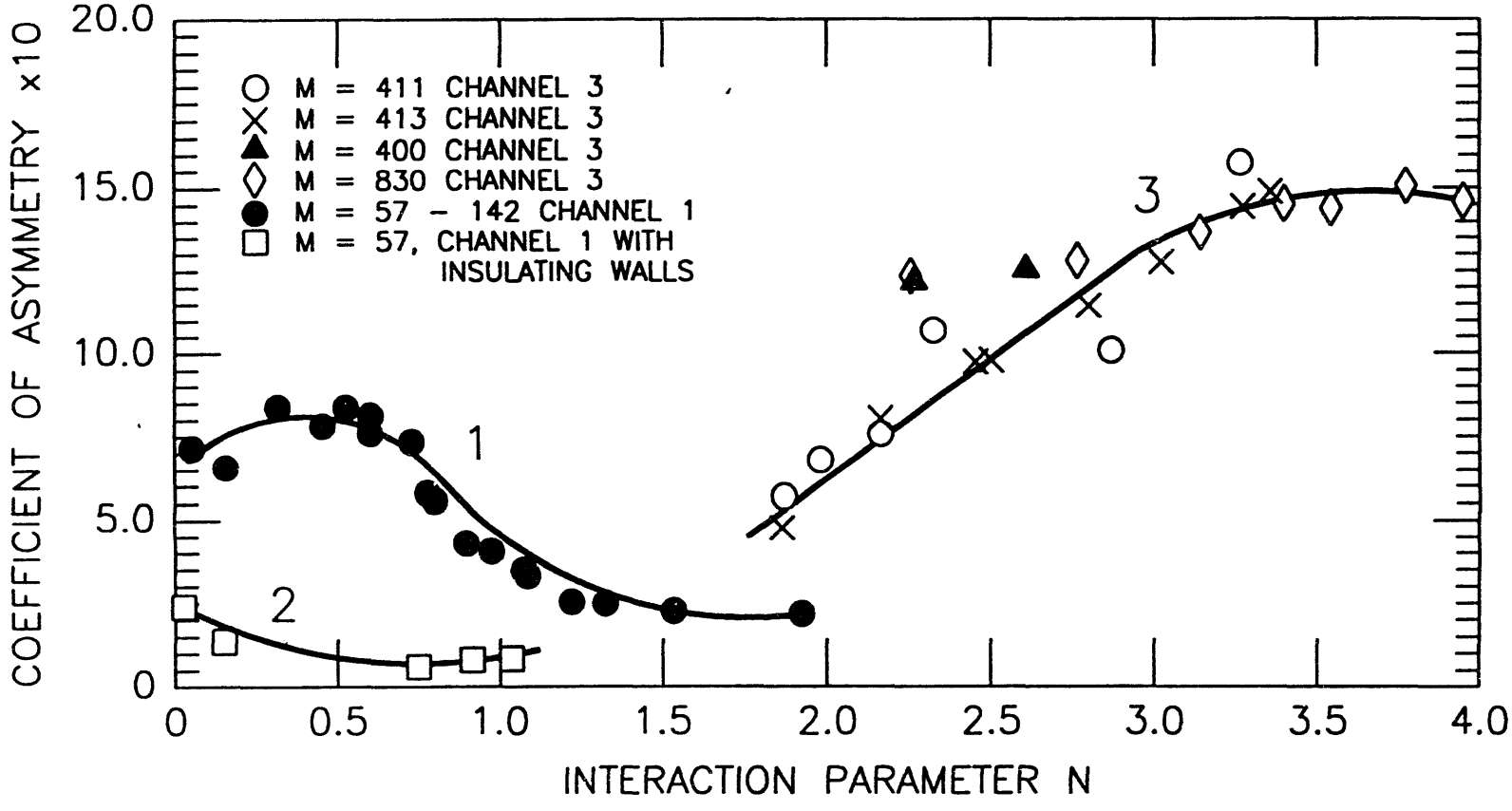

FIGURE 7

G10182

20A

Fig. 9

DATE
FILMED
11/17/94

END